JACS
JOURNAL OF THE AMERICAN CHEMICAL SOCIETY
Article
Cite This: J. Am. Chem. Soc. 2018, 140, 2528−2536
pubs.acs.org/JACS

Catalytic Silylation of N_2 and Synthesis of NH_3 and N_2H_4 by Net Hydrogen Atom Transfer Reactions Using a Chromium P_4 Macrocycle

Alexander J. Kendall, Samantha I. Johnson, R. Morris Bullock, and Michael T. Mock*

Center for Molecular Electrocatalysis, Pacific Northwest National Laboratory, P.O. Box 999, Richland, Washington 99352, United States

Supporting Information

ABSTRACT: We report the first discrete molecular Cr-based catalysts for the reduction of N_2. This study is focused on the reactivity of the Cr-N_2 complex, *trans*-$[Cr(N_2)_2(P^{Ph}{}_4N^{Bn}{}_4)]$ ($\mathbf{P_4Cr(N_2)_2}$), bearing a 16-membered tetraphosphine macrocycle. The architecture of the [16]-$P^{Ph}{}_4N^{Bn}{}_4$ ligand is critical to preserve the structural integrity of the catalyst. $\mathbf{P_4Cr(N_2)_2}$ was found to mediate the reduction of N_2 at room temperature and 1 atm pressure by three complementary reaction pathways: (1) Cr-catalyzed reduction of N_2 to $N(SiMe_3)_3$ by Na and Me_3SiCl, affording up to 34 equiv $N(SiMe_3)_3$; (2) stoichiometric reduction of N_2 by protons and electrons (for example, the reaction of cobaltocene and collidinium triflate at room temperature afforded 1.9 equiv of NH_3, or at −78 °C afforded a mixture of NH_3 and N_2H_4); and (3) the first example of NH_3 formation from the reaction of a terminally bound N_2 ligand with a traditional H atom source, TEMPOH (2,2,6,6-tetramethylpiperidine-1-ol). We found that *trans*-$[Cr(^{15}N_2)_2(P^{Ph}{}_4N^{Bn}{}_4)]$ reacts with excess TEMPOH to afford 1.4 equiv of $^{15}NH_3$. Isotopic labeling studies using TEMPOD afforded ND_3 as the product of N_2 reduction, confirming that the H atoms are provided by TEMPOH.

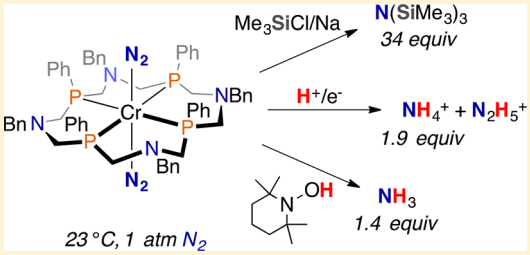

INTRODUCTION

The development of catalysts for N_2 reduction to NH_3 is a vital area of energy research to reduce the enormous infrastructure, energy input, and CO_2 emissions of the industrial Haber−Bosch process that generates the critical supply of NH_3 used in agriculture and industry.[1] The emergence of NH_3 as a promising energy carrier for H_2 storage or use in direct NH_3 fuel cells[2] also motivates the investigation of small-scale processes for the synthesis of NH_3 from N_2. Robust molecular electrocatalysts could provide the necessary selectivity for N_2 reduction to NH_3 over thermodynamically preferred H^+ reduction to H_2 when utilizing protons and electrons.[3] Such advances may lead to small-scale, decentralized, CO_2-free NH_3 production facilities with protons and electrons derived from renewable resources.

Drawing inspiration from biological N_2 fixation with protons and electrons carried out by the multimetallic active sites of the nitrogenase enzymes,[4] well-defined synthetic complexes based on Fe,[5] Mo,[6] and Co[7] have recently emerged as catalysts for N_2 reduction to NH_3 and N_2H_4 using Brønsted acids and chemical reductants such as metallocenes or KC_8. While the N_2 reduction mechanism had commonly been thought to proceed through a series of H^+/e^- transfer steps, Peters and co-workers recently proposed that N−H bond-forming reactions may follow proton-coupled electron transfer (PCET) pathways through the formation of protonated metallocenes.[5d] PCET pathways[8] could invoke hydrogen atom transfer (HAT) to M-N_2 and M-N_xH_y intermediates en route to NH_3 formation. While PCET pathways using separate acids and reductants have been demonstrated, NH_3 formation from a M-N_2 complex by concerted delivery of H^+/e^- as a hydrogen atom ($H^\bullet$) from a hydrogen atom donor such as TEMPOH remains elusive.

The reduction of N_2 to silylamines is a complementary approach for NH_3 production, where NH_3 can be attained by subsequent treatment of the silylamine product with acid (Figure 1, eq 1).[9] Studies describing the N_2 silylation mechanism suggest that silyl radicals,[10] generated *in situ* from Me_3SiCl and Na, K, or KC_8, react with a M-N_2 species to form

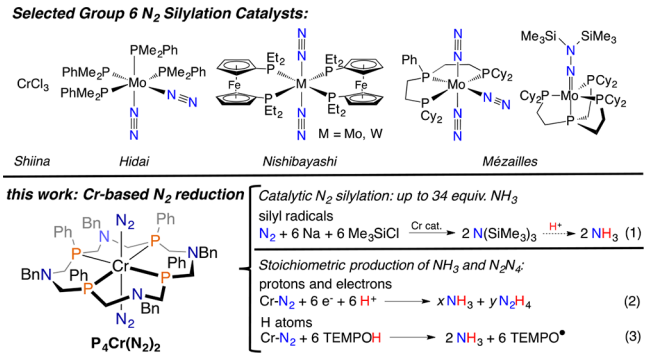

Figure 1. Top: Selected group 6 complexes shown to catalyze the reduction of N_2 to $N(SiMe_3)_3$. Bottom: N_2 reduction reactions examined in this work with $\mathbf{P_4Cr(N_2)_2}$.

Received: October 24, 2017
Published: January 31, 2018

DOI: 10.1021/jacs.7b11132
J. Am. Chem. Soc. 2018, 140, 2528−2536

N−Si bonds. The seminal 1972 report by Shiina revealed $CrCl_3$ to be the first transition metal salt to catalyze this reaction, forming 5.4 equiv of N_2-derived tris(trimethylsilyl)amine, $N(SiMe_3)_3$, using Li as the reducing agent.[11]

Since that early account, several homogeneous catalytic systems using first-row transition metals such as Fe,[10b,12] Co,[12d,13] and V[14] have been reported; of the group 6 metals, several molecular Mo^0-N_2 precursors and one W^0-N_2 complex bearing phosphine ligands catalyze N_2 silylation (Figure 1, top).[10a,c,15] Even though solvated $CrCl_3$ displayed notable reactivity to catalyze N_2 reduction 45 years ago, only one example of Cr-mediated N_2 cleavage has been subsequently reported.[16] No discrete molecular Cr catalysts for N_2 reduction are currently known. Notably, two reported attempts to utilize Cr with multidentate ligand platforms that afforded Mo-based N_2 reduction catalysts did not lead to Cr catalysts.[15c,17] In both cases, the targeted Cr-N_2 complex was not attained. These examples underscore the challenge of synthesizing stable Cr complexes for N_2 reduction and the divergence of chemical behavior Cr displays compared with analogous well-studied congeners. Therefore, Cr complexes have the potential to provide group 6 metal-N_2 reduction chemistry that is distinct from Mo and W.

Our interest in Cr for N_2 reduction originated with the discovery of isolable Cr-N_2 complexes containing $P^{Ph}{}_nN^{Bn}{}_n$ ligands (n = 2, 3, or 4).[18] In particular, *trans*-$[Cr(^{15}N_2)_2(P^{Ph}{}_4N^{Bn}{}_4)]$, $\mathbf{P_4Cr(^{15}N_2)_2}$, bearing a 16-membered macrocycle (Figure 1, bottom panel) affords $^{15}N_2$-derived $^{15}N_2H_5^+$ and $^{15}NH_4^+$ upon reaction with triflic acid at −50 °C.[18b] Thus, $\mathbf{P_4Cr(N_2)_2}$, with the notable kinetic and thermodynamic macrocyclic stability of a tetraphosphine macrocycle,[19] inspired our efforts to investigate Cr for catalytic N_2 reduction. Herein we report the first molecular Cr complexes for the catalytic conversion of N_2 to silylamines, (Figure 1, eq 1). Our studies focus on the reactivity of $\mathbf{P_4Cr(N_2)_2}$ that affords up to 34 equiv of $N(SiMe_3)_3$ per Cr center. The unique 16-membered phosphorus macrocycle is critical to preserve the structural integrity of the catalyst, allowing the homogeneous complex to maintain its catalytic activity and to be recycled, producing substantial catalytic formation of $N(SiMe_3)_3$ upon substrate reloading. In this study, we establish the reactivity of $\mathbf{P_4Cr(N_2)_2}$ at room temperature with protons *and* electrons (Figure 1, eq 2) and consider the role of PCET pathways in the production of up to 1.9 equiv of NH_3 or a mixture of NH_3 and N_2H_4. Lastly, the reactivity of $\mathbf{P_4Cr(^{15}N_2)_2}$ with TEMPOH (2,2,6,6-tetramethylpiperidine-1-ol) to form $^{15}N_2$-derived $^{15}NH_3$ (Figure 1, eq 3) is presented, providing the first experimental evidence for NH_3 formation directly from a terminally bound N_2 ligand using a traditional hydrogen atom donor.

■ RESULTS AND DISCUSSION

Structure, Stability, and N_2 Binding of $P_4Cr(N_2)_2$. The macrocyclic complex $\mathbf{P_4Cr(N_2)_2}$ was prepared using a modified synthetic procedure developed since our initial report,[18b] and it was isolated as an orange crystalline solid in 21% yield. In Figure 2, we recount the molecular structure of $\mathbf{P_4Cr(N_2)_2}$ that was reported in our prior study from X-ray crystallography to illustrate the relationship between the structure of $\mathbf{P_4Cr(N_2)_2}$ enforced by the all-*syn*-isomer of the [16]-$P^{Ph}{}_4N^{Bn}{}_4$ ligand and the high stability of the complex. We have noted the difficulty in forming discrete Cr^0-N_2 complexes with chelating phosphine ligands compared to Mo and W analogues.[20] Our own attempts have given a handful of stable Cr^0-N_2 complexes in low to

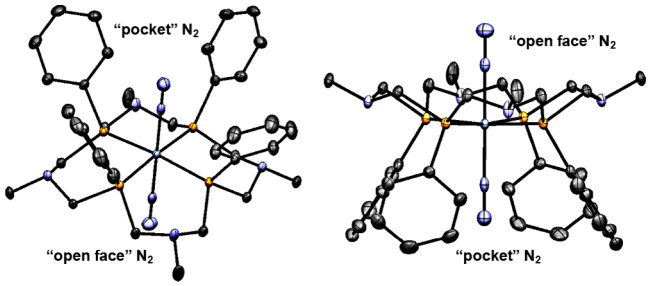

Figure 2. Top and side views of the molecular structure of $\mathbf{P_4Cr(N_2)_2}$, highlighting the contrasting steric environments around the N_2 ligands. Only the benzyl carbon atoms of NBn groups are shown for clarity.

moderate yields, and we found that the intrinsic geometric constraints of some bidentate and tetradentate phosphine ligands greatly impact stability; i.e., the complexes are thermally sensitive toward N_2 ligand loss at Cr^0 or could not be attained (see Supporting Information (SI), Table S1).[18c] For example, our attempts to prepare a Cr^0-N_2 complex with the tetradentate $P^{Ph}{}_4N^{Ph}{}_2$ ligand[12c] resulted in a thermally sensitive $Cr^0(N_2)_2$ species despite the rigid, but distorted, planar and meridonal P_4 coordination environment. In a second example, the complex $Cr(N_2)(dmpe)(P^{Ph}{}_3N^{Bn}{}_3)$, entry 3 in Table 1, is a remarkably stable Cr-N_2 complex formed in high yield when using dmpe ($Me_2PCH_2H_2PMe_2$) as the bidentate ligand. In contrast, $Cr(N_2)(dmpm)(P^{Ph}{}_3N^{Bn}{}_3)$ could not be attained using dmpm ($Me_2PCH_2PMe_2$), a diphosphine with a smaller bite angle. While it is not surprising that the ligand chelate effect increases complex stability,[21] Cr^0 seems far more sensitive to ligand bite angles than Mo, especially in the latter example where diphosphines with a single carbon atom in the backbone have been used extensively to support P_5Mo-N_2 complexes.[22] Consequently, an apparently critical core geometric parameter we have noted as a general trend to attain stable Cr-N_2 complexes is P−P ligand bite angles that are close to 90°, affording an archetypal octahedral coordination environment for Cr. In the present case, a main contributor to the high stability of the complex is the P−P bond angles of the [16]-$P^{Ph}{}_4N^{Bn}{}_4$ ligand, 89.7° and 90.0°, giving Cr a nearly perfect octahedral geometry with the two axial N_2 ligands.

Inherent to the $\mathbf{P_4Cr(N_2)_2}$ structure are the contrasting steric environments above and below the P_4Cr plane in which the N_2 ligands reside (Figure 2). One N_2 ligand occupies a "pocket" formed by the four phenyl substituents on P, and the opposing N_2 ligand is in a comparatively open face of the macrocycle. Accordingly, these contrasting environments impact the strength of N_2 binding to Cr, which we believe contributes to catalytic reactivity. We evaluated the N_2 binding affinities by Density Functional Theory (DFT) analysis (methods in the Supporting Information) and found that the "pocket" N_2 ligand exhibits a lower dissociation energy (11.0 kcal/mol) compared to the N_2 ligand in the open face (20.7 kcal/mol). As discussed below, we propose that N_2 dissociation is a required step before catalysis; thus, based upon this computational assessment of the N_2 binding affinities, the N_2 functionalization occurs at the open face N_2 ligand.

Catalytic Reduction of N_2 to $N(SiMe_3)_3$. The reaction of $\mathbf{P_4Cr(N_2)_2}$ with 100 equiv of Na and Me_3SiCl at 1 atm N_2 and room temperature yielded 10.6 turnovers of $N(SiMe_3)_3$ (TON = turnover number = N atoms/Cr). The $N(SiMe_3)_3$ that was produced was identified by GC-MS and then acidified to give

DOI: 10.1021/jacs.7b11132
J. Am. Chem. Soc. 2018, 140, 2528−2536

Table 1. Catalytic Reduction of N_2 to $N(SiMe_3)_3$ Using Cr Complexes

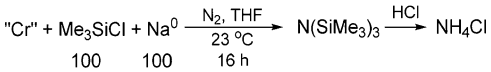

Entry	Cr complex[a]	ν_{NN} (cm^{-1})	equiv NH_4Cl[b]
1	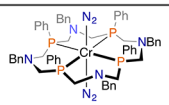 **$P_4Cr(N_2)_2$**	1918, 2072 (THF)	10.6 17.1[c] 21.2[c,d] 34.1[e]
2	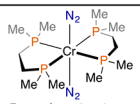 *trans*-$[Cr(N_2)_2(dmpe)_2]$	1932 (hexane[23])	5.2
3	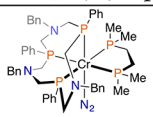 $Cr(N_2)(dmpe)(P^{Ph}{}_3N^{Bn}{}_3)$	1918 (THF[18c])	6.2
4	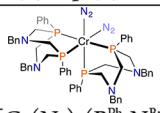 *cis*-$[Cr(N_2)_2(P^{Ph}{}_2N^{Bn}{}_2)_2]$	1937, 2009 (THF[18a])	4.8
5	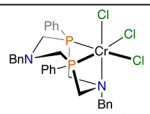 *fac*-$[CrCl_3(\kappa^3\text{-}(P,P,N)P^{Ph}{}_2N^{Bn}{}_2)]$	-	6.8
6	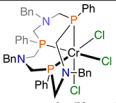 *fac*-$[CrCl_3(P^{Ph}{}_3N^{Bn}{}_3)]$	-	5.0
7	$Cr(CO)_6$	-	4.8
8	$Cr(C_6H_6)(CO)_3$	-	3.8
9	$Cr(C_6H_6)_2$	-	0.2
10	$CrCl_2(THF)$	-	<0.1
11[f]	$CrCp_2$	-	4.4
12[g]	$CrCp^*{}_2$	-	1.9
13	$CrCl_3(THF)_3$	-	0.5
14	$CrBr_3(THF)_3$	-	2.5
15	Cr powder	-	<0.1
16	None	-	<0.1

[a]["Cr"] = 10^{-4} M, 23 °C, 1 atm N_2. [b]All values reported are an average of at least two trials. [c]Silylated glassware, 1.0 M Me_3SiCl (10^5 equiv), and 10^5 equiv of Na. [d]Run 72 h. [e]Run 16 h, refreshed with another 1.0 M Me_3SiCl (10^5 equiv) and an equivalent amount of Na, and run an additional 16 h. [f]Cp = C_5H_5. [g]Cp* = $C_5(CH_3)_5$.

NH_4Cl that was quantified by ^1H NMR spectroscopy, in which 64% of the electrons went into reducing N_2 (Table 1, entry 1). Higher TONs were achieved by increasing the loading of Na and Me_3SiCl up to 10^5 equiv/Cr, yielding up to 21.2 TON in a single run. After a catalytic run was complete, the mixture can be directly replenished (or filtered and replenished) with fresh reagents, and $\mathbf{P_4Cr(N_2)_2}$ continues to catalytically reduce N_2 to $N(SiMe_3)_3$, with yields doubling from 17.1 TON (first loading) to 34.1 TON (combined total after second loading). The observed TONs do not appear to scale linearly with reagent concentration—likely caused by the heterogeneous nature of Na and active radical species concentration in a constant flux (see proposed mechanism below). Catalytic N_2 reduction with homogeneous complexes is notoriously sensitive to reaction conditions to achieve catalysis,[5d] especially the solvent.[5a,b,14] Accordingly, we screened a variety of experimental conditions in our catalytic N_2 silylation studies of $\mathbf{P_4Cr(N_2)_2}$, including silane identity, reductant, solvent, and temperature. The results of these catalytic trials are listed in the SI, Tables S2−S5.

A variety of molecular chromium complexes and Cr-salts were examined to determine the generality of N_2 reduction by Cr (Table 1). Surprisingly, several of the chromium complexes that were tested exhibited TONs comparable to those in the initial report by Shiina.[11] In fact, nine of the 14 chromium salts or complexes yielded TON over 2, with all Cr entries yielding at least a trace amount of reduced N_2 product. This extensive test of Cr-based compounds more clearly demonstrates the activity of Cr for N_2 reduction, regardless of whether the compounds have a N_2 ligand. Similar catalytic activity has been observed for Fe complexes that do not bind a N_2 ligand at room temperature.[10b,12b]

For the Cr complexes containing N_2 ligands, there does not appear to be a correlation between N_2 activation, as measured by the ν_{NN} bands in the infrared spectrum, and catalyst TON under the conditions in Table 1. The $\mathbf{P_4Cr(N_2)_2}$ complex was unique among this group in that it produced the highest TONs, was recyclable, and exists as a molecular species during and after catalysis (see below). All other chromium salts and complexes displayed rapid Cr^0 precipitation out of solution. For instance, reactions run with *trans*-$[Cr(N_2)_2(dmpe)_2]$[23] yielded free dmpe ligand by ^{31}P NMR spectroscopy. Based on these observations, it is likely that the reduction and oxidation of chromium, specifically Cr^0 to Cr^I oxidation states, represent a soft/hard transition[24] and cause ligand lability. It is proposed that once a chromium species is oxidized in the cycle for N_2 reduction, ligand dissociation leads to metal aggregation and observable precipitation. Thus, we infer that it is the Cr-ligand stability over redox cycles, not only the activation of N_2, that leads to catalytic turnover.

Multidentate phosphine ligand strategies have been pursued for N_2 reduction by Tuczek and co-workers to prevent ligand loss at high metal oxidation states of Mo.[22a,b,25] For Cr, geometry-optimized multidentate ligand systems are imperative for mere stability. The $\mathbf{P_4Cr(N_2)_2}$ complex is resilient to ligand dissociation; in fact, we have not observed ligand loss as a pathway of catalyst deactivation in this study. The $\mathbf{P_4Cr(N_2)_2}$ remains molecularly discrete and in solution during the redox cycling necessary for catalytic turnover.[26]

To illustrate this point, we compared the catalytic reactivity of $\mathbf{P_4Cr(N_2)_2}$ (Table 1, entry 1) to those of *trans*-$[Cr(N_2)_2(dmpe)_2]$ (Table 1, entry 2) and *cis*-$[Cr(N_2)_2(P^{Ph}{}_2N^{Bn}{}_2)_2]$ (Table 1, entry 4). *trans*-$[Cr(N_2)_2(dmpe)_2]$ is most structurally similar to $\mathbf{P_4Cr(N_2)_2}$, while *cis*-$[Cr(N_2)_2(P^{Ph}{}_2N^{Bn}{}_2)_2]$ is a structural isomer of $\mathbf{P_4Cr(N_2)_2}$. In reactions performed with increased loading of silane and reductant, 10^5 equiv of Na, and 10^5 equiv of Me_3SiCl (SI, Table S8), both *trans*-$[Cr(N_2)_2(dmpe)_2]$ and *cis*-$[Cr(N_2)_2(P^{Ph}{}_2N^{Bn}{}_2)_2]$ performed almost identically to the results in Table 1, while $\mathbf{P_4Cr(N_2)_2}$ afforded almost double the TON of $N(SiMe_3)_3$. In addition, *trans*-$[Cr(N_2)_2(dmpe)_2]$ and *cis*-$[Cr(N_2)_2(P^{Ph}{}_2N^{Bn}{}_2)_2]$ could be not be recycled to generate additional $N(SiMe_3)_3$ as illustrated with $\mathbf{P_4Cr(N_2)_2}$. Because of the electronic and structural similarities

DOI: 10.1021/jacs.7b11132
J. Am. Chem. Soc. 2018, 140, 2528−2536

of these complexes, the striking divergence in reactivity is assigned to the macrocyclic effect of the ligand—specifically the ability to maintain chromium as a molecular species during the redox cycling, N_2 reduction, and catalysis.

Mechanistic Considerations for Silylation Catalysis with $P_4Cr(N_2)_2$. To improve our understanding of the mechanism and speciation of the reaction components formed during catalysis, the catalytic reaction was examined after 8 h, before complete consumption of the Na and Me_3SiCl reagents at 16 h. Upon analysis of the reaction mixture by GC-MS and ^1H NMR spectroscopy, a better picture of the reaction profile emerged. In addition to the $N(SiMe_3)_3$ generated from N_2 reduction, the only organic reaction products were $(Me_3Si)_2$, trimethyl(4-(trimethylsilyl)butoxy)silane, and an insoluble polymer of THF (Figure 3). The formation of these organic

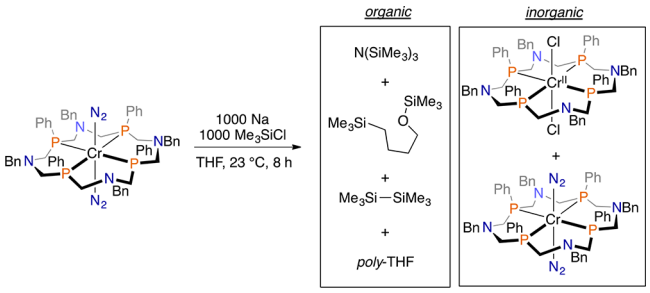

Figure 3. Organic and inorganic reaction products identified after 8 h of catalysis with $P_4Cr(N_2)_2$ during the reduction of N_2 to $N(SiMe_3)_3$. Organic products were identified by ^1H NMR spectroscopy and GC-MS analysis; inorganic products were identified by ^1H and ^{31}P NMR spectroscopy and single-crystal X-ray diffraction.

products, which have been reported previously,[10c,15a,b] supports the *in situ* generation of $SiMe_3$ radicals in solution, formed from the reaction of Na with Me_3SiCl. Consequently, the reaction of $SiMe_3$ radicals with THF, and the homocoupling reaction, represent significant side reactions that reduce the concentration of $SiMe_3$ radicals in solution, thus competing kinetically with N_2 reduction process.

The identity of the inorganic reaction products was determined by NMR spectroscopy. After reacting for 8 h, $P_4Cr(N_2)_2$ was observed in the reaction mixture by ^{31}P NMR spectroscopy. In addition, a paramagnetic species in the ^1H NMR spectrum was isolated as yellow crystals and identified by single-crystal X-ray diffraction matched the previously reported complex *trans*-$[Cr(Cl)_2(P^{Ph}{}_4N^{Bn}{}_4)]$ ($P_4Cr^{II}(Cl)_2$).[18b] Most importantly, no free ligand was observed in the reaction mixture by ^{31}P NMR spectroscopy, indicating that the macrocycle remained intact. Independently, we confirmed that $P_4Cr^{II}(Cl)_2$ can be directly generated from the reaction of $P_4Cr(N_2)_2$ with Me_3SiCl in THF (Figure 4). To further confirm the identity of the isolated paramagnetic Cr^{II} species

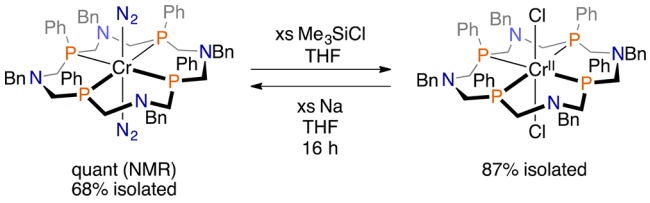

Figure 4. Independent verification of observed inorganic products during catalytic reduction of N_2 to $N(SiMe_3)_3$.

and to understand its reactivity under catalytic conditions, the isolated $P_4Cr^{II}(Cl)_2$ was reacted with excess Na to cleanly yield $P_4Cr(N_2)_2$, reaching full conversion after 16 h. The slow rate of reduction of $P_4Cr^{II}(Cl)_2$ by Na metal to generate $P_4Cr(N_2)_2$ is likely due to the heterogeneous reduction conditions. Based on the independent reactivity of these two complexes, it is likely that their individual concentrations are in constant flux during catalysis. Importantly, the clean reduction to continuously regenerate $P_4Cr(N_2)_2$ from $P_4Cr^{II}(Cl)_2$ and Na allows the Cr complex to be recycled upon substrate reloading.

To enhance catalytic TON, reactions were performed under increased N_2 pressure (90 atm). Unexpectedly, $P_4Cr(N_2)_2$ consistently failed to produce more than 4.1 TON using the same reaction conditions that afforded 17.2 TON at 1 atm N_2 (SI, Table S7). The deleterious effect of N_2 pressure on catalysis is surprising, as we anticipated that increasing the concentration of dissolved N_2 in solution would enhance catalysis by favoring N_2 binding during catalytic turnover. Indeed, this result contrasts with the 4-fold *increase* in TON we observed upon increasing the N_2 pressure from 1 to 100 atm in the catalytic reduction of N_2 to $N(SiMe_3)_3$ using $Fe^0(N_2)$-$(P_4{}^{Ph}N^{Ph}{}_2)$.[12c] Intuitively, this suggested to us that dissociation of one N_2 ligand to a generate a putative 5-coordinate "$P_4Cr^0(N_2)$" complex is a prerequisite for catalysis. Hidai and co-workers have proposed a similar initial step of dissociation of N_2 from *cis*-$[Mo(N_2)_2(PMe_2Ph)_4]$ prior to subsequent N_2 reduction.[27] In our previously described protonation mechanism of $P_4Cr(N_2)_2$, the dissociation of one N_2 was determined by DFT calculations to increase the proton affinity of the bound N_2 to enable N−H bond formation. The lability of N_2 is also the likely cause of the previously reported irreversible $Cr^{I/0}$ redox couple at slow scan rates by cyclic voltammetry.[18b]

Based on the results of the catalytic trials, the independent reactivity of $P_4Cr(N_2)_2$ and $P_4Cr^{II}(Cl)_2$, and insights from related group 6 catalysts,[10,15b,28] we propose a mechanism for catalytic reduction of N_2 to silylamines by $P_4Cr(N_2)_2$ (Figure 5). The proposed mechanism initiates with $P_4Cr(N_2)_2$:

(a) Upon mixing, a background reaction is established between the two Cr species, Me_3SiCl, and Na.

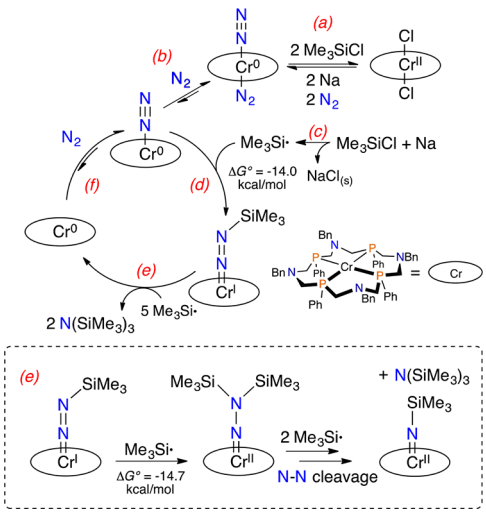

Figure 5. Proposed catalytic cycle for $P_4Cr(N_2)_2$ reducing N_2 to $N(SiMe_3)_3$. The proposed intermediates listed in the box for the steps shown as (e) were obtained from DFT calculations; see SI for details.

DOI: 10.1021/jacs.7b11132
J. Am. Chem. Soc. 2018, 140, 2528−2536

(b) After the dissociation of the "in-pocket" N_2 ligand, a 5-coordinate $P_4Cr^0(N_2)$ complex enters the catalytic cycle.

(c) Concomitantly, $SiMe_3$ radicals are generated *in situ* from the reaction of Na and Me_3SiCl. The $SiMe_3$ radicals are presumed to be the active species in catalysis; however, the concentration of $SiMe_3$ radicals available to react with Cr-N_2 can be affected by the rate of $(Me_3Si)_2$ formation and reactions with THF as shown above.

(d) The $SiMe_3$ radical reacts with the distal N atom of N_2, initiating an oxidation state change of Cr. DFT calculations predict that this reaction is favorable by 14 kcal/mol. The resistance of the "$\mathbf{P_4Cr}$" fragment to phosphine ligand dissociation at this stage is believed to be critical to prevent Cr^0 precipitation.

(e) The silylated intermediates formed in subsequent reaction steps have not been identified experimentally. However, DFT calculations suggest that the second added $SiMe_3$ radical is thermodynamically favored to react at the distal nitrogen atom by 14.7 kcal/mol, forming a silylhydrazido intermediate. The lack of phosphine ligand dissociation of the macrocycle favors this intermediate over silyl radical addition at the proximal nitrogen atom. DFT predicts that the addition of a third silyl radical leads to N−N bond cleavage, generating $N(SiMe_3)_3$ and a P_4Cr-N-$SiMe_3$ species that undergoes further reactions with silyl radicals to produce the second equivalent of $N(SiMe_3)_3$. A similar reaction mechanism in a recent Mo-based N_2 silylation catalyst was described by Mézailles and co-workers and was supported by several isolated and structurally characterized intermediates.[10a] On the basis of the bonding description of reduced Cr-N_xH_y intermediates from H^+ and e^- additions by DFT computations,[18b,c] the formation of a silylhydrazine $(Me_3Si)_2NN(SiMe_3)_2$ product is plausible; however, the steric bulk of the $SiMe_3$ groups and the necessary (but unlikely) dissociation of a phosphine atom from Cr disfavors this N_2 silylation pathway.

(f) Under reducing conditions, P_4Cr^0 is regenerated, and the coordination of N_2 to chromium completes the catalytic cycle.

Reduction of N_2 to NH_3 Using Protons and Electrons. In addition to studying $\mathbf{P_4Cr(N_2)_2}$ reactivity with silyl radicals, we examined the reaction of $\mathbf{P_4Cr(N_2)_2}$ with various sources of protons and electrons for the reduction of N_2 directly to NH_3; the results are summarized in Table 2. Protonated metallocenes that serve as PCET reagents or effective H atom sources for N_2 reduction[5d] may exhibit one-electron radical-based reactivity with $\mathbf{P_4Cr(N_2)_2}$, similar to reactions with silyl radicals. In our experiments, $\mathbf{P_4Cr(N_2)_2}$ was added to a freshly prepared solution of 40 equiv of acid and 30 equiv of reductant in THF. In reactions performed at room temperature $\mathbf{P_4Cr(N_2)_2}$ generated 1.9 equiv of NH_4^+ using cobaltocene ($CoCp_2$) as the reductant (−1.33 V vs $Cp_2Fe^{0/+}$ in THF),[29] and collidinium triflate (ColH[OTf]) as a proton source (Table 2, entry 1). The reducing strength of $CoCp_2$ is only ∼100 mV more negative than the quasi-reversible $E_{1/2}$ value for the $Cr^{I/0}$ couple of $\mathbf{P_4Cr(N_2)_2}$ at −1.22 V vs $Cp_2Fe^{0/+}$ in THF.[18b] Interestingly, the formation of NH_4^+ from N_2 at room temperature displays a clear dependence on the reduction potential of the metallocene. For example, no reduced N_2 products were observed at room temperature with stronger reductants such as decamethylcobaltocene ($CoCp^*_2$) (−1.98 V vs $Cp_2Fe^{0/+}$ in THF),[5a] or decamethylchromocene ($CrCp^*_2$) (−1.55 V vs $Cp_2Fe^{0/+}$ in THF).[31a] In addition, chromocene ($CrCp_2$) (−1.07 V vs $Cp_2Fe^{0/+}$ in CH_3CN)[31b] was ineffective at affording reduced N_2 products, although this may be due to its inability to reduce Cr to the Cr^0 oxidation state. At room temperature, it is possible that competing side reactions, such as H_2 evolution,[6c,32] between the stronger reducing agents and ColH[OTf] occur rapidly, before productive N−H bond formation. This is particularly likely if N_2 dissociation from $\mathbf{P_4Cr(N_2)_2}$ is a prerequisite step before initiating reactivity at N_2. Reactions with $CoCp^*_2$ and ColH[OTf] conducted at −78 °C further support this hypothesis, as 1.3 equiv of NH_4^+ was formed by initially lowering the reaction temperature (Table 2, entry 8).

Table 2. Direct Synthesis of NH_4^+ and $N_2H_5^+$ from $P_4Cr(N_2)_2$, Protons, and a Reducing Agent

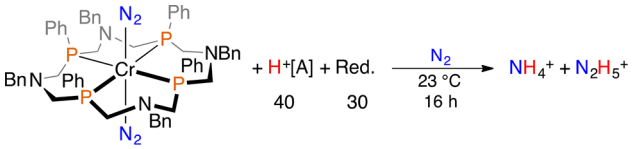

entry[a]	reductant[b]	acid[c]	solvent	NH_4^+[d]	$N_2H_5^+$[e]
1	$CoCp_2$	ColH[OTf]	THF	1.9	<0.1
2	$CoCp^*_2$	ColH[OTf]	THF	<0.1	<0.1
3	$CrCp_2$	ColH[OTf]	THF	<0.1	<0.1
4	$CrCp^*_2$	ColH[OTf]	THF	<0.1	<0.1
5	$CoCp_2$	Ph_2NH_2[OTf]	THF	0.7	0.4
6[f]	$CoCp_2$	ColH[OTf]	THF	0.7	<0.1
7[g]	$CoCp_2$	ColH[OTf]	THF	0.6	0.2
8[g]	$CoCp^*_2$	ColH[OTf]	THF	1.3	<0.1
9	$CoCp_2$	ColH[OTf]	toluene	<0.1	<0.1
10	$CoCp_2$	ColH[OTf]	pentane	0.3	0.1
11	$CoCp_2$	ColH[OTf]	PhF	0.5	0.2
12	$CoCp_2$	ColH[OTf]	Et_2O	0.1	0.4

[a]Run at 0.1 mM [Cr], 23 °C, 16 h. [b]Cp = C_5H_5, Cp* = $C_5(CH_3)_5$ [c]Col = 2,4,6-trimethylpyridine, OTf = trifluoromethanesulfonate. [d]Equivalents of NH_4^+ quantified using ^{1}H NMR spectroscopy. [e]Equivalents of $N_2H_5^+$ quantified using *p*-dimethylaminobenzaldehyde test.[30] [f]Run at 55 °C. [g]Run at −78 °C for 4 h, and then slowly warmed to 23 °C for 8 h.

Though catalytic turnover was not observed with $\mathbf{P_4Cr(N_2)_2}$ using the current combination of acid, counteranion, reductant, and solvent, $N_2H_5^+$ was detected and quantified in several trials. Perhaps most striking is the comparison between entries 1 and 7 in Table 2, wherein $N_2H_5^+$ is observed when the reaction is initially conducted at −78 °C before warming to room temperature for 8 h. These results suggest that at lower temperatures an alternating N_2 reduction pathway[33] is occurring at Cr, where the first two N−H bonds are formed at the distal and proximal nitrogen atoms, respectively. The alternating N−H bond formation would eventually lead to the formation of hydrazine, which was observed in several cases (Table 2). The observation of N_2H_4 as a product in the reaction implicates P_4Cr-N_2H_4 as a possible reaction intermediate in the complete reduction of N_2 to NH_3. Although it is not conclusive that NH_3 formation proceeds via N_2H_4 directly,[34] we observed $N_2H_5^+$ at room temperature in entries 5 and 12 using the weaker acid Ph_2NH_2[OTf] or less polar solvent, respectively.[35] Because $N_2H_5^+$ is observed at low temperature in a reaction that yields exclusively NH_4^+ at room temperature, and $N_2H_5^+$ is observed in several other reactions

DOI: 10.1021/jacs.7b11132
J. Am. Chem. Soc. 2018, 140, 2528−2536

that also yield ammonia, it is likely that N_2H_4 is an intermediate in the mechanism of reduction from N_2 to NH_3.

In a series of control experiments focusing on the separate reactivity of $\mathbf{P_4Cr(N_2)_2}$ with ColH[OTf] and $CoCp_2$, we discovered that $\mathbf{P_4Cr(N_2)_2}$ did not react with either of these reagents independently. When 8 equiv of ColH[OTf] was mixed with $\mathbf{P_4Cr(N_2)_2}$ over several days in a sealed NMR tube, no observable reactivity was noted, as determined by the absence of free collidine, absence of paramagnetic features, no H_2 formation, and unchanged ^{1}H and ^{31}P NMR spectra of $\mathbf{P_4Cr(N_2)_2}$ (Figure S5). The stability of $\mathbf{P_4Cr(N_2)_2}$ in the presence of ColH[OTf] was also investigated by in situ IR spectroscopy, showing the vibrational frequency of the symmetric and asymmetric ν_{NN} bands remain unchanged after acid addition (Figure S4). The lack of reactivity between $\mathbf{P_4Cr(N_2)_2}$ and ColH[OTf] is surprising because low-valent molecular N_2 coordination complexes typically exhibit a very basic metal center and are susceptible to protonation at the metal to form metal hydrides, especially with ligand platforms containing pendant amine groups.[20a,b,36] Typically this pervasive H^+ reduction event must be mitigated by low concentrations of acid or insoluble acids for N_2 reduction.[5d,6a] The long-term acid stability of $\mathbf{P_4Cr(N_2)_2}$ toward ColH[OTf] must be due to poor kinetics for proton transfer since H_2 formation is thermodynamically favorable. $\mathbf{P_4Cr(N_2)_2}$ lacks accessible cis-coordination sites to N_2 which would otherwise provide a more facile route to proton reduction and H_2 formation. Moreover, the four phenyl groups of the P_4 ligand offer steric protection from bulky acids such as ColH[OTf] from effectively transferring a proton to the face of the complex most likely to have dissociated a N_2 ligand.

Addition of $CoCp_2$ to a THF-d_8 solution of ColH[OTf] and $\mathbf{P_4Cr(N_2)_2}$ at room temperature led to an immediate reaction as indicated by the appearance of free collidine, changing paramagnetic features, and H_2 in the ^{1}H NMR spectrum.[37] Because $\mathbf{P_4Cr(N_2)_2}$ was not observed to react with $CoCp_2$ or ColH[OTf] independently, but reacts (to yield NH_4^+) when *both* reagents are present, either an intermediate species (between $CoCp_2$ and ColH[OTf]) or ternary system is required for N_2 reduction. A ternary system would not be kinetically favorable given the dilute conditions. Alternatively, a protonated metallocene ($CoCp_2H$[OTf]) or pyridinyl radicals[38] (ColH$^\bullet$) from the reduction of pyridinium acids, are two plausible intermediate species that could be generated in situ that exhibit bond dissociation free energies (BDFEs) optimal for PCET or HAT reactivity with coordinated N_2. Because the proton source and electron source must both be present in solution for reactivity with $\mathbf{P_4Cr(N_2)_2}$, a PCET pathway must be operating in the initial reductive steps from N_2 to NH_3. Based on the known BDFEs of $CoCp_2H$[OTf] and ColH$^\bullet$, HAT is a plausible mechanism.[5d]

To further assess one-electron radical-based reactivity for the synthesis of NH_3 from N_2 by hydrogen atom transfer pathways, we investigated the reaction of $\mathbf{P_4Cr(N_2)_2}$ with a traditional organic HAT reagent 2,2,6,6-tetramethylpiperidin-1-ol (TEMPOH). Related reactions of TEMPOH with M-nitride complexes have been reported. For example, in a study from Smith and co-workers, HAT steps were proposed in the stoichiometric synthesis of NH_3 from the reaction of excess TEMPOH with a terminal iron(IV) nitride complex.[39] Similarly, Schneider and co-workers proposed HAT in the formation of an Ir-NH_2 complex from the reaction of an Ir-nitride complex with excess TEMPOH.[40] Lastly, Holland and co-workers formed NH_3 from the reaction of 2,4,6-tri-*tert*-butylphenol with a N_2-derived tetrairon bis(nitride) complex.[41] However, to our knowledge, NH_3 formation from the reaction of TEMPOH with a terminally bound N_2 molecule is unprecedented.

Treatment of $\mathbf{P_4Cr(N_2)_2}$ with 100 equiv of TEMPOH affords 1.4 equiv of free NH_3, which was vacuum transferred directly out of the reaction flask (without any additives), then quantified by ^{1}H NMR spectroscopy upon acidification of the NH_3 gas in a separate vessel (see SI for details).[42] Hydrazine was not detected as a product in this reaction, and the reaction of $\mathbf{P_4Cr(N_2)_2}$ with 87 equiv of TEMPO radical produced no NH_3 (SI, Figure S10). Importantly, we confirmed the ammonia that is generated originates from the reduction of the dinitrogen ligands, as the reaction of excess TEMPOH with $\mathbf{P_4Cr(^{15}N_2)_2}$ affords $^{15}NH_4^+$, as observed by ^{1}H NMR spectroscopy (SI, Figure S9). In addition, we have established the origin of the hydrogen atoms in the formation of ammonia from reduction of the terminally bound N_2 ligand by reacting $\mathbf{P_4Cr(^{15}N_2)_2}$ with excess TEMPOD in protio THF. Treatment of $\mathbf{P_4Cr(^{15}N_2)_2}$ with 100 equiv of TEMPOD at room temperature affords $^{15}ND_3$, which was identified as a broad singlet at 0.65 ppm by ^{2}H NMR spectroscopy (SI, Figure S11). In an NMR tube experiment, the reaction of $\mathbf{P_4Cr(N_2)_2}$ with excess TEMPOH yields unidentified paramagnetic products by ^{1}H NMR spectroscopy, and no signals were observed in the ^{31}P NMR spectrum. The effort to identify the final Cr-containing product of this NH_3 forming reaction is ongoing; these observations suggest the P_4N_4 ligand has remained intact and oxidation of $\mathbf{P_4Cr(N_2)_2}$ has occurred (SI, Figure S7). Since TEMPO radical was not observed as a product, it is plausible that NH_3 generation is accompanied by the concomitant formation of Cr−O bonds,[43] akin to the Fe-(TEMPO) product formed in the reactions of the Fe^{IV}-nitride with TEMPOH by Smith and co-workers.[39a]

Given that excess ColH[OTf] did not react independently with $\mathbf{P_4Cr(N_2)_2}$, proton transfer from the weakly acidic TEMPOH ($pK_a \approx 41$ in CH_3CN)[44] is not expected to be thermodynamically accessible (although the electron-rich $\mathbf{P_4Cr(^{15}N_2)_2}$ *has* been shown to react with HOTf to form $^{15}NH_4^+$ and $^{15}N_2H_5^+$). Furthermore, based on the redox properties of TEMPOH ($E_{1/2}$ = 0.71 V in CH_3CN)[45] electron transfer to $\mathbf{P_4Cr(N_2)_2}$ ($Cr^{I/0} = -1.22$ V vs $Cp_2Fe^{0/+}$ in THF; no reduction wave was observed for $\mathbf{P_4Cr(N_2)_2}$ up to −2.5 V in THF) is also an unlikely initial step. While the complete balance of products formed in this transformation is not defined at this time, the reaction of TEMPOH with $\mathbf{P_4Cr(N_2)_2}$ to form N−H bonds of NH_3 shows the plausibility that concerted hydrogen atom transfers are occurring directly with a terminally bound N_2 ligand. Because we have not yet identified the final Cr-containing product, we cannot rigorously rule out N_2 reduction by heterolytic pathways. While the labeling studies have unambiguously established $^{15}N_2$ and TEMPOD as the sources of nitrogen and hydrogen atoms, respectively, in the *net* hydrogen atom transfer reactions to form ammonia, this description of the overall reaction does not require that the reaction proceed by a single-step HAT mechanism.

■ CONCLUSION

We report the first molecular chromium complexes capable of catalytic N_2 reduction. These Cr complexes catalytically reduce N_2 to silylamines at room temperature and pressure, with the

DOI: 10.1021/jacs.7b11132
J. Am. Chem. Soc. 2018, 140, 2528−2536

macrocycle-containing complex $\mathbf{P_4Cr(N_2)_2}$ affording up to 34 equiv of $N(SiMe_3)_3$ per Cr. $\mathbf{P_4Cr(N_2)_2}$ is also capable of stoichiometric reduction of nitrogen with H^+ and e^- or with TEMPOH. Most Cr species screened in this study showed some activity toward N_2 reduction. The low TONs observed with almost all Cr species studied can be explained by the inability of the Cr complexes to remain in solution when undergoing redox chemistry necessary for catalysis, with reactions typically resulting in $Cr^0_{(s)}$ precipitating out of solution (with observed free ligand in solution). The key structural feature to achieving higher turnover and even recyclability of a catalyst was a tetradentate macrocyclic ligand, affording long lifetimes in solution.

Direct synthesis of NH_4^+ and $N_2H_5^+$ from N_2 was achieved, though catalytic N_2 reduction with protons and electrons was not observed with the current scope of reagents examined in this study. Notably, $N_2H_5^+$ was detected in several cases, suggesting that N_2H_4 is a reduction intermediate and the Cr complex proceeds through an alternating N_2 reduction pathway that diverges from analogous Mo- and W-N_2 reduction chemistry. $\mathbf{P_4Cr(N_2)_2}$ does not react directly with the acid or the reductant used in these reactions. Rather, it is very likely that an intermediate species is generated *in situ* from the $CoCp_2$ reductant and the ColH[OTf] acid that performs HAT to $\mathbf{P_4Cr(N_2)_2}$, the details of which are currently under investigation. We more clearly demonstrated the likelihood of HAT using TEMPOH as a hydrogen atom source to produce free NH_3 directly from N_2.

In these cases, both independent electron transfer and proton transfer are unlikely initial mechanistic pathways for N−H bond formation due to thermodynamic or kinetic barriers, implying HAT for the initial step. Isotopic labeling (e.g., $^{15}N_2$ and TEMPOD) unambiguously distinguishes the sources of N and H for NH_3 formation, further corroborating this interpretation.

Though some details of this reaction are not currently understood, the proof of principle for a HAT mechanism for N_2 reduction of NH_3 directly at room temperature and pressure has been demonstrated. This work supports the notion that HAT can have significant advantages over stepwise H^+/e^- pathways, and both Cr complexes and HAT mechanisms will play a key role in homogeneous N_2 reduction in the future.

■ EXPERIMENTAL SECTION

All synthetic procedures were performed under an atmosphere of N_2 using standard Schlenk or glovebox techniques. Reactions performed with $^{15}N_2$ gas were subsequently handled in the glovebox under an atmosphere of argon. Unless described otherwise, all reagents were purchased from commercial sources and were used as received. Protio solvents were dried by passage through activated alumina columns in an Innovative Technology, Inc., PureSolv solvent purification system and stored under N_2 or argon until use. Virgin glassware was used without surface modification. Acid-washed glassware was prepared by washing virgin glassware with 12.1 M HCl overnight at room temperature. Silylated glassware was prepared by washing virgin glassware with concentrated HCl overnight at room temperature and then silylating following the literature procedure using Me_2SiHCl.[46] All glassware was heated to 160 °C overnight before use.

All ^1H, ^{13}C, ^{15}N, and ^{31}P NMR spectra were collected in thin-walled NMR tubes on a Varian Inova or NMR S 500 MHz spectrometer at 25 °C unless otherwise indicated. ^2H NMR spectra were recorded on a Varian NMR S 300 MHz spectrometer at 25 °C in non-deuterated THF. ^1H and ^{13}C NMR chemical shifts are referenced to residual protio solvent resonances in the deuterated solvent. ^{31}P NMR chemical shifts are proton decoupled unless otherwise noted and referenced to 85% H_3PO_4 ($\delta = 0$) as an external reference. ^{15}N NMR chemical shifts are referenced to $CH_3{}^{15}NO_2$ ($\delta = 0$) as an external reference.

Infrared spectra were recorded on a Thermo Scientific Nicolet iS10 FT-IR spectrometer as a KBr pellet under a purge stream of nitrogen gas. In situ IR experiments were performed in a nitrogen-filled glovebox and recorded on a Mettler-Toledo ReactIR 15 spectrometer equipped with a liquid-nitrogen-cooled MCT detector, connected to a 1.5 m AgX Fiber DS series (9.5 mm × 203 mm) probe with a silicon sensor. $^{15}N_2$ (98%) gas and THF-d_8 were purchased from Cambridge Isotope Labs. THF- d_8 was dried over NaK and vacuum transferred before use. Magnesium powder was purchased from Rieke Metals LLC and used as received. All chromium reagents were purchased and used as received. A procedure for the synthesis of $\mathbf{P_4Cr(N_2)_2}$ is described in the SI. Chromium complexes examined for silylation catalysis were prepared from literature procedures as described in the SI. TEMPOH, purchased from Cambridge Chemicals, was dissolved in pentane, filtered, and vacuum-dried to ensure complete removal of water. TEMPOD was synthesized using a modified preparation for TEMPOH, with acetone-d_6 and D_2O replacing the non-deutero reagents.[47]

Me_3SiCl was purified by refluxing overnight over CaH_2 under N_2, followed by an air-free fractional distillation yielding >99.9% pure Me_3SiCl by ^1H NMR. Sodium sand was prepared by taking sodium metal (20 g) in dodecane (250 mL) and refluxing with vigorous stirring under N_2. (***Caution!*** *Use a heating mantle and grease all joints thoroughly.*) Once the sodium liquid dispersion formed a fine particulate, the stirring was halted, and the vessel was slowly cooled back to room temperature, yielding a fine sodium sand. The solid was collected by filtration on a frit in a glovebox, washed with THF followed by pentane, and dried under reduced pressure, yielding ultrafine sodium sand. $P^{Ph}{}_2N^{Bn}{}_2$ was prepared according to the literature preparation of $P^{Ph}{}_2N^{tBu}{}_2$ with the modification that $BnNH_2$ was used instead of $^tBuNH_2$. Note that very slow addition of $BnNH_2$ is recommended because the reaction is exothermic.[48]

Procedure for Cr-Catalyzed Reduction of N_2 to $N(SiMe_3)_3$. A solution of Me_3SiCl and reductant was stirred for 5 min in THF. To this mixture was added the chromium complex as a THF solution. The mixture was stirred for 8−72 h. The reaction mixture was then filtered thorough Celite and rinsed thoroughly with additional THF. The filtrate was acidified with 1000 equiv of HCl in Et_2O (1 M, 1.5 mL), and the solvent was evaporated, giving a solid. To the residue was added 0.500 mL of a stock solution of 8.5 mM 1,3,5-trimethoxybenzene (TMB) in DMSO-d_6. The resulting solution was analyzed by ^1H NMR spectroscopy with the relaxation delay set to 10 s based on the longest T_1 relaxation measurement of 1.4 s for the TMB aromatic proton. ^1H NMR spectroscopy showed the diagnostic NH_4^+ peak at 7.29 ppm (1:1:1 triplet, J = 50.9 Hz), quantified versus TMB.

Procedure for Reduction of N_2 to NH_4^+ with $P_4Cr(N_2)_2$ Using Protons and Electrons. First, 40 equiv of solid acid was added to 30 equiv of solid reductant in a specialized vacuum transfer Schlenk flask (SI, Figure S1). To this mixture was added solvent followed by $\mathbf{P_4Cr(N_2)_2}$ (10 μL from a 10 mM stock solution, 0.1 μmol delivery) in either THF or toluene. The vessel was quickly sealed under 1 atm of N_2 and stirred overnight at 23 °C. Following the protocol described Ashley and co-workers,[5a] the mixture was quenched with HCl etherate (500 equiv), and volatiles were removed under reduced pressure. While frozen at −196 °C, 40 wt%/wt $KOH_{(aq)}$ was added to the solids. In the collection bulb attached to the reaction bulb, HCl etherate was frozen as well. The apparatus was evacuated under a high vacuum and sealed. The reaction bulb was warmed to room temperature for the vacuum transfer of NH_3 gas to the frozen acidified bulb. Upon warming, the acidified bulb was thoroughly mixed, the solvent was removed under reduced pressure, and ^1H NMR spectroscopic analysis as described above was used to quantify NH_4Cl. The reaction bulb was re-acidified with concentrated $HCl_{(aq)}$ and tested for hydrazinium using the procedure described by Ashley and co-workers[5a] and the *p*-dimethylaminobenzaldehyde test.[30]

Procedure for Reduction of N_2 to NH_4^+ with $P_4Cr(N_2)_2$ Using TEMPOH. First, 100 equiv of solid TEMPOH was added into a

DOI: 10.1021/jacs.7b11132
J. Am. Chem. Soc. 2018, 140, 2528−2536

specialized vacuum transfer Schlenk flask (SI, Figure S1). To this mixture was added THF followed by $\mathbf{P_4Cr(N_2)_2}$ in THF (see above). The vessel was quickly sealed under 1 atm of N_2 and stirred overnight at 23 °C. In a collection bulb attached to the reaction bulb, HCl etherate was frozen. The reaction bulb was also frozen. The apparatus was evacuated under a high vacuum and sealed. The reaction bulb was warmed to room temperature for the volatiles to vacuum transfer to the frozen acidified bulb. Upon warming, the acidified bulb was thoroughly mixed, solvent was removed under reduced pressure, and ^{1}H NMR spectral analysis as above was used to quantify NH_4Cl. The reaction bulb was acidified with concentrated $HCl_{(aq)}$ and tested for hydrazinium using the procedure described by Ashley and co-workers[5a] and the *p*-dimethylaminobenzaldehyde test.[30]

Procedure for the Reduction of N_2 to ND_3 Using TEMPOD. First, 100 equiv of solid TEMPOD was added to a J. Young NMR tube. A solution of $\mathbf{P_4Cr(N_2)_2}$ in protio THF was then added, and the tube was quickly sealed and thoroughly mixed. The resulting orange-brown solution was analyzed by ^{2}H NMR spectroscopy. A diagnostic broad singlet resonance at 0.65 ppm was identified as the free ND_3 product.

■ ASSOCIATED CONTENT

Supporting Information

The Supporting Information is available free of charge on the ACS Publications website at DOI: 10.1021/jacs.7b11132.

Detailed experimental procedures, computational details, quantification methods, NMR spectra, and selected experiments (PDF)

■ AUTHOR INFORMATION

Corresponding Author

*michael.mock@pnnl.gov

ORCID

R. Morris Bullock: 0000-0001-6306-4851

Michael T. Mock: 0000-0002-7310-2791

Notes

The authors declare no competing financial interest.

■ ACKNOWLEDGMENTS

This research was supported as part of the Center for Molecular Electrocatalysis, an Energy Frontier Research Center funded by the U.S. Department of Energy (DOE), Office of Science, Office of Basic Energy Sciences. PNNL is operated by Battelle for the U.S. DOE. The authors thank Dr. Geoffrey Chambers for the single-crystal X-ray diffraction identification of $P_4Cr^{II}(Cl)_2$ and Dr. Eric Wiedner for helpful discussions.

■ REFERENCES

(1) (a) Smil, V. *Enriching the Earth: Fritz Haber, Carl Bosch, and the Transformation of World Food Production*; MIT Press: Cambridge, MA, 2001. (b) Kandemir, T.; Schuster, M. E.; Senyshyn, A.; Behrens, M.; Schlögl, R. *Angew. Chem., Int. Ed.* **2013**, *52*, 12723−12726. (c) Roundhill, D. M. *Chem. Rev.* **1992**, *92*, 1−27. (d) Erisman, J. W.; Sutton, M. A.; Galloway, J.; Klimont, Z.; Winiwarter, W. *Nat. Geosci.* **2008**, *1*, 636−639. (e) Smil, V. *Nature* **1999**, *400*, 415.

(2) (a) Lindley, B. M.; Appel, A. M.; Krogh-Jespersen, K.; Mayer, J. M.; Miller, A. J. M. *ACS Energy Lett.* **2016**, *1*, 698−704. (b) Lan, R.; Irvine, J. T. S.; Tao, S. *Int. J. Hydrogen Energy* **2012**, *37*, 1482−1494. (c) Schüth, F.; Palkovits, R.; Schlögl, R.; Su, D. S. *Energy Environ. Sci.* **2012**, *5*, 6278−6289.

(3) Singh, A. R.; Rohr, B. A.; Schwalbe, J. A.; Cargnello, M.; Chan, K.; Jaramillo, T. F.; Chorkendorff, I.; Nørskov, J. K. *ACS Catal.* **2017**, *7*, 706−709.

(4) (a) Seefeldt, L. C.; Hoffman, B. M.; Dean, D. R. *Annu. Rev. Biochem.* **2009**, *78*, 701−722. (b) Hoffman, B. M.; Lukoyanov, D.; Yang, Z. Y.; Dean, D. R.; Seefeldt, L. C. *Chem. Rev.* **2014**, *114*, 4041−4062. (c) Lukoyanov, D.; Khadka, N.; Yang, Z.-Y.; Dean, D. R.; Seefeldt, L. C.; Hoffman, B. M. *J. Am. Chem. Soc.* **2016**, *138*, 10674−10683.

(5) (a) Hill, P. J.; Doyle, L. R.; Crawford, A. D.; Myers, W. K.; Ashley, A. E. *J. Am. Chem. Soc.* **2016**, *138*, 13521−13524. (b) Kuriyama, S.; Arashiba, K.; Nakajima, K.; Matsuo, Y.; Tanaka, H.; Ishii, K.; Yoshizawa, K.; Nishibayashi, Y. *Nat. Commun.* **2016**, *7*, 12181. (c) Buscagan, T. M.; Oyala, P. H.; Peters, J. C. *Angew. Chem., Int. Ed.* **2017**, *56*, 6921−6926. (d) Chalkley, M. J.; Del Castillo, T. J.; Matson, B. D.; Roddy, J. P.; Peters, J. C. *ACS Cent. Sci.* **2017**, *3*, 217−223. (e) Del Castillo, T. J.; Thompson, N. B.; Peters, J. C. *J. Am. Chem. Soc.* **2016**, *138*, 5341−5350. (f) Anderson, J. S.; Rittle, J.; Peters, J. C. *Nature* **2013**, *501*, 84−87. (g) Creutz, S. E.; Peters, J. C. *J. Am. Chem. Soc.* **2014**, *136*, 1105−1115.

(6) (a) Yandulov, D. V.; Schrock, R. R. *Science* **2003**, *301*, 76−78. (b) Arashiba, K.; Miyake, Y.; Nishibayashi, Y. *Nat. Chem.* **2011**, *3*, 120−125. (c) Kuriyama, S.; Arashiba, K.; Nakajima, K.; Tanaka, H.; Kamaru, N.; Yoshizawa, K.; Nishibayashi, Y. *J. Am. Chem. Soc.* **2014**, *136*, 9719−9731. (d) Arashiba, K.; Kinoshita, E.; Kuriyama, S.; Eizawa, A.; Nakajima, K.; Tanaka, H.; Yoshizawa, K.; Nishibayashi, Y. *J. Am. Chem. Soc.* **2015**, *137*, 5666−5669. (e) Wickramasinghe, L. A.; Ogawa, T.; Schrock, R. R.; Muller, P. *J. Am. Chem. Soc.* **2017**, *139*, 9132−9135. (f) Kuriyama, S.; Arashiba, K.; Nakajima, K.; Tanaka, H.; Yoshizawa, K.; Nishibayashi, Y. *Chem. Sci.* **2015**, *6*, 3940−3951. (g) Eizawa, A.; Arashiba, K.; Tanaka, H.; Kuriyama, S.; Matsuo, Y.; Nakajima, K.; Yoshizawa, K.; Nishibayashi, Y. *Nat. Commun.* **2017**, *8*, 14874. (h) Tanabe, Y.; Nishibayashi, Y. *Chem. Rec.* **2016**, *16*, 1549−1577. (i) Tanabe, Y.; Arashiba, K.; Nakajima, K.; Nishibayashi, Y. *Chem. - Asian J.* **2018**, *12*, 2544−2548.

(7) Kuriyama, S.; Arashiba, K.; Tanaka, H.; Matsuo, Y.; Nakajima, K.; Yoshizawa, K.; Nishibayashi, Y. *Angew. Chem., Int. Ed.* **2016**, *55*, 14291−14295.

(8) (a) Lindley, B. M.; Bruch, Q. J.; White, P. S.; Hasanayn, F.; Miller, A. J. M. *J. Am. Chem. Soc.* **2017**, *139*, 5305−5308. (b) Pappas, I.; Chirik, P. J. *J. Am. Chem. Soc.* **2015**, *137*, 3498−3501. (c) Pappas, I.; Chirik, P. J. *J. Am. Chem. Soc.* **2016**, *138*, 13379−13389. (d) Matson, B. D; Peters, J. C. *ACS Catal.* **2018**, *8*, 1448−1455. (e) Bezdek, M.; Chirik, P. J. *Angew. Chem. Int. Ed.* **2018**, DOI: 10.1002/anie.201708406.

(9) (a) Burford, R. J.; Fryzuk, M. D. *Nat. Rev. Chem.* **2017**, *1*, 0026. (b) Duman, L. M.; Sita, L. R. *J. Am. Chem. Soc.* **2017**, *139*, 17241−17244.

(10) (a) Liao, Q.; Saffon-Merceron, N.; Mézailles, N. *ACS Catal.* **2015**, *5*, 6902−6906. (b) Yuki, M.; Tanaka, H.; Sasaki, K.; Miyake, Y.; Yoshizawa, K.; Nishibayashi, Y. *Nat. Commun.* **2012**, *3*, 1254. (c) Tanaka, H.; Sasada, A.; Kouno, T.; Yuki, M.; Miyake, Y.; Nakanishi, H.; Nishibayashi, Y.; Yoshizawa, K. *J. Am. Chem. Soc.* **2011**, *133*, 3498−3506.

(11) Shiina, K. *J. Am. Chem. Soc.* **1972**, *94*, 9266−9267.

(12) (a) Araake, R.; Sakadani, K.; Tada, M.; Sakai, Y.; Ohki, Y. *J. Am. Chem. Soc.* **2017**, *139*, 5596−5606. (b) Ung, G.; Peters, J. C. *Angew. Chem., Int. Ed.* **2014**, *54*, 532−535. (c) Prokopchuk, D. E.; Wiedner, E. S.; Walter, E. D.; Popescu, C. V.; Piro, N. A.; Kassel, W. S.; Bullock, R. M.; Mock, M. T. *J. Am. Chem. Soc.* **2017**, *139*, 9291−9301. (d) Imayoshi, R.; Nakajima, K.; Takaya, J.; Iwasawa, N.; Nishibayashi, Y. *Eur. J. Inorg. Chem.* **2017**, 3769−3778.

(13) (a) Siedschlag, R. B.; Bernales, V.; Vogiatzis, K. D.; Planas, N.; Clouston, L. J.; Bill, E.; Gagliardi, L.; Lu, C. C. *J. Am. Chem. Soc.* **2015**, *137*, 4638−4641. (b) Imayoshi, R.; Tanaka, H.; Matsuo, Y.; Yuki, M.; Nakajima, K.; Yoshizawa, K.; Nishibayashi, Y. *Chem. - Eur. J.* **2015**, *21*, 8905−8909. (c) Gao, Y.; Li, G.; Deng, L. *J. Am. Chem. Soc.* **2018**, *140*, 2239.

(14) Imayoshi, R.; Nakajima, K.; Nishibayashi, Y. *Chem. Lett.* **2017**, *46*, 466−468.

(15) (a) Liao, Q.; Saffon-Merceron, N.; Mézailles, N. *Angew. Chem., Int. Ed.* **2014**, *53*, 14206−14210. (b) Komori, K.; Oshita, H.; Mizobe, Y.; Hidai, M. *J. Am. Chem. Soc.* **1989**, *111*, 1939−1940. (c) Kuriyama,

DOI: 10.1021/jacs.7b11132
J. Am. Chem. Soc. 2018, 140, 2528−2536

S.; Arashiba, K.; Nakajima, K.; Tanaka, H.; Yoshizawa, K.; Nishibayashi, Y. *Eur. J. Inorg. Chem.* **2016**, *2016*, 4856−4861.
(16) Vidyaratne, I.; Scott, J.; Gambarotta, S.; Budzelaar, P. H. M. *Inorg. Chem.* **2007**, *46*, 7040−7049.
(17) Smythe, N. C.; Schrock, R. R.; Müller, P.; Weare, W. W. *Inorg. Chem.* **2006**, *45*, 7111−7118.
(18) (a) Mock, M. T.; Chen, S.; Rousseau, R.; O'Hagan, M. J.; Dougherty, W. G.; Kassel, W. S.; DuBois, D. L.; Bullock, R. M. *Chem. Commun.* **2011**, *47*, 12212−12214. (b) Mock, M. T.; Chen, S.; O'Hagan, M.; Rousseau, R.; Dougherty, W. G.; Kassel, W. S.; Bullock, R. M. *J. Am. Chem. Soc.* **2013**, *135*, 11493−11496. (c) Mock, M. T.; Pierpont, A. W.; Egbert, J. D.; O'Hagan, M.; Chen, S.; Bullock, R. M.; Dougherty, W. G.; Kassel, W. S.; Rousseau, R. *Inorg. Chem.* **2015**, *54*, 4827−4839. (d) Egbert, J. D.; O'Hagan, M.; Wiedner, E. S.; Bullock, R. M.; Piro, N. A.; Kassel, W. S.; Mock, M. T. *Chem. Commun.* **2016**, *52*, 9343−9346. (e) Bhattacharya, P.; Prokopchuk, D. E.; Mock, M. T. *Coord. Chem. Rev.* **2017**, *334*, 67−83.
(19) Swor, C. D.; Tyler, D. R. *Coord. Chem. Rev.* **2011**, *255*, 2860−2881.
(20) (a) Labios, L. A.; Heiden, Z. M.; Mock, M. T. *Inorg. Chem.* **2015**, *54*, 4409−4422. (b) Weiss, C. J.; Egbert, J. D.; Chen, S.; Helm, M. L.; Bullock, R. M.; Mock, M. T. *Organometallics* **2014**, *33*, 2189−2200. (c) Weiss, C. J.; Groves, A. N.; Mock, M. T.; Dougherty, W. G.; Kassel, W. S.; Helm, M. L.; DuBois, D. L.; Bullock, R. M. *Dalton Trans.* **2012**, *41*, 4517−4529.
(21) Karsch, H. H. *Angew. Chem., Int. Ed. Engl.* **1977**, *16*, 56−57.
(22) (a) Broda, H.; Hinrichsen, S.; Krahmer, J.; Nather, C.; Tuczek, F. *Dalton Trans.* **2014**, *43*, 2007−2012. (b) Broda, H.; Krahmer, J.; Tuczek, F. *Eur. J. Inorg. Chem.* **2014**, *2014*, 3564−3571. (c) Söncksen, L.; Gradert, C.; Krahmer, J.; Nather, C.; Tuczek, F. *Inorg. Chem.* **2013**, *52*, 6576−6589.
(23) Girolami, G. S.; Salt, J. E.; Wilkinson, G.; Thornton-Pett, M.; Hursthouse, M. B. *J. Am. Chem. Soc.* **1983**, *105*, 5954−5956.
(24) (a) Huheey, J. E.; Keiter, E. A.; Keiter, R. L.; Medhi, O. K. *Inorganic Chemistry: Principles of Structure and Reactivity*; Pearson Education: South Asia, 2006. (b) Theopold, K. H. *Encyclopedia of Inorganic Chemistry*; John Wiley & Sons, Ltd.: New York, 2006.
(25) (a) Hinrichsen, S.; Kindjajev, A.; Adomeit, S.; Krahmer, J.; Nather, C.; Tuczek, F. *Inorg. Chem.* **2016**, *55*, 8712−8722. (b) Hinrichsen, S.; Schnoor, A. C.; Grund, K.; Floser, B.; Schlimm, A.; Nather, C.; Krahmer, J.; Tuczek, F. *Dalton. Trans.* **2016**, *45*, 14801−14813.
(26) Note that throughout this study, whenever $\mathbf{P_4Cr(N_2)_2}$ was used for reaction chemistry, no free ligand was observed. Further, no other Cr source (including insoluble Cr salts and Cr powder) yielded equally high turnovers, and the $\mathbf{P_4Cr(N_2)_2}$ catalyst was equally active after submicrometer filtration. These results suggest that a heterogeneous Cr species is unlikely to be responsible for the significant increase in N_2 reduction efficacy when using the macrocyclic ligand.
(27) Hidai, M.; Mizobe, Y. *Chem. Rev.* **1995**, *95*, 1115−1133.
(28) Liao, Q.; Cavaillé, A.; Saffon-Merceron, N.; Mézailles, N. *Angew. Chem., Int. Ed.* **2016**, *55*, 11212−11216.
(29) Schrock, R. R. *Acc. Chem. Res.* **2005**, *38*, 955−962.
(30) Watt, G. W.; Chrisp, J. D. *Anal. Chem.* **1952**, *24*, 2006−2008.
(31) (a) Fajardo, J., Jr.; Peters, J. C. *J. Am. Chem. Soc.* **2017**, *139*, 16105−16108. (b) Holloway, J. D. L.; Geiger, W. E. *J. Am. Chem. Soc.* **1979**, *101*, 2038−2044.
(32) Koelle, U.; Infelta, P. P.; Grätzel, M. *Inorg. Chem.* **1988**, *27*, 879−883.
(33) Tyler, D. R.; Balesdent, C. G.; Kendall, A. J. In *Comprehensive Inorganic Chemistry II*, 2nd ed.; Reedijk, J., Poeppelmeier, K., Eds.; Elsevier: Amsterdam, 2013; pp 525−552.
(34) Note that a distal mechanism (ref 32) that proceeds through a nitride intermediate cannot currently be ruled out, which is proposed with other group 6 N_2 complexes. See ref 6f and the following: Schrock, R. R. *Angew. Chem., Int. Ed.* **2008**, *47*, 5512−5522. It is also possible that liberated hydrazine is further reduced or has undergone disproportionation to form NH_4^+.
(35) Solubility limitations of $[N_2H_5][OTf]$, as reported by Ashley and co-workers (ref 5a), could contribute to the observation of $N_2H_5^+$ because the species is forced out of solution before complete reduction occurs.
(36) (a) Creutz, S. E.; Peters, J. C. *Chem. Sci.* **2017**, *8*, 2321−2328. (b) Labios, L. A.; Weiss, C. J.; Egbert, J. D.; Lense, S.; Bullock, R. M.; Dougherty, W. G.; Kassel, W. S.; Mock, M. T. *Z. Anorg. Allg. Chem.* **2015**, *641*, 105−117.
(37) Note that $CoCp_2$ and ColH[OTf] slowly react to produce H_2 under these conditions over several hours, based on a $CoCp_2$ color change from orange to light yellow.
(38) Bezdek, M. J.; Pappas, I.; Chirik, P. J. *Top. Organomet. Chem.* **2017**, *60*, 1−21.
(39) (a) Scepaniak, J. J.; Young, J. A.; Bontchev, R. P.; Smith, J. M. *Angew. Chem., Int. Ed.* **2009**, *48*, 3158−3160. (b) Smith, J. M.; Subedi, D. *Dalton Trans.* **2012**, *41*, 1423−1429.
(40) Scheibel, M. G.; Abbenseth, J.; Kinauer, M.; Heinemann, F. W.; Wurtele, C.; de Bruin, B.; Schneider, S. *Inorg. Chem.* **2015**, *54*, 9290−9302.
(41) MacLeod, K. C.; McWilliams, S. F.; Mercado, B. Q.; Holland, P. L. *Chem. Sci.* **2016**, *7*, 5736−5746.
(42) We found that $\mathbf{P_4Cr(N_2)_2}$ does not readily react with only stoichiometric quantities (1−6 equiv) of TEMPOH. However, ND_3 was detected by ^2H NMR spectroscopy upon treatment of $\mathbf{P_4Cr(N_2)_2}$ with 47 equiv of TEMPOD.
(43) For additional examples of M-TEMPO complexes see: (a) Liu, Y.-L.; Kehr, G.; Daniliuc, C. G.; Erker, G. *Organometallics* **2017**, *36*, 3407−3414. (b) Huang, K.-W.; Han, J. H.; Cole, A. P.; Musgrave, C. B.; Waymouth, R. M. *J. Am. Chem. Soc.* **2005**, *127*, 3807−3816. (c) Nguyen, T. A.; Wright, A. M.; Page, J. S.; Wu, G.; Hayton, T. W. *Inorg. Chem.* **2014**, *53*, 11377−11387. (d) Kleinlein, C.; Bendelsmith, A. J.; Zheng, S. L.; Betley, T. A. *Angew. Chem., Int. Ed.* **2017**, *56*, 12197−12201.
(44) Mader, E. A.; Manner, V. W.; Markle, T. F.; Wu, A.; Franz, J. A.; Mayer, J. M. *J. Am. Chem. Soc.* **2009**, *131*, 4335−4345.
(45) Warren, J. J.; Tronic, T. A.; Mayer, J. M. *Chem. Rev.* **2010**, *110*, 6961−7001.
(46) Armarego, W. L. F.; Chai, C. L. L. *Purification of Laboratory Chemicals*; Elsevier: London, 2003.
(47) Mader, E. A.; Davidson, E. R.; Mayer, J. M. *J. Am. Chem. Soc.* **2007**, *129*, 5153−5166.
(48) Franz, J. A.; O'Hagan, M.; Ho, M.-H.; Liu, T.; Helm, M. L.; Lense, S.; DuBois, D. L.; Shaw, W. J.; Appel, A. M.; Raugei, S.; Bullock, R. M. *Organometallics* **2013**, *32*, 7034−7042.

DOI: 10.1021/jacs.7b11132
J. Am. Chem. Soc. 2018, 140, 2528−2536